

Self-referenced spectral interferometry

T. Oksenhendler · S. Coudreau · N. Forget ·
V. Crozatier · S. Grabielle · R. Herzog · O. Gobert ·
D. Kaplan

Received: 22 June 2009 / Revised version: 3 November 2009 / Published online: 6 February 2010
© Springer-Verlag 2010

Abstract A new femtosecond pulse characterization, named self-referenced spectral interferometry, is introduced. Based on linear spectral interferometry, the reference pulse is self created from the pulse being characterized. This self reference results from pulse shaping optimization and non-linear temporal filtering.

1 Introduction

A pulse is fully determined by its spectral amplitude and phase. The spectral phase is usually expanded into a Taylor series whose absolute and first terms correspond to absolute phase and delay, which are not relevant for pulse characterization.

As demonstrated by Wong and Walmsley [1], in the absence of any reference pulse, the complete temporal characterization of femtosecond pulses requires a non-linear or non-stationary filter.

The most widely used pulse measurement techniques, frequency-resolved optical gating (FROG) [2] and spectral phase interferometry for direct electric-field reconstruction (SPIDER) [3], indeed rely on three-wave or four-wave mixing processes to generate a signal from which the spectral phase can be retrieved. Both these techniques are self referenced and can be made single shot by the use of

non-collinear harmonic generation. However, the algorithms used to retrieve the spectral complex amplitude are not straightforward. FROG, for instance, belongs to the class of spectrographic measurement and relies on a blind iterative retrieval algorithm [4]. With the SPIDER technique, an analytic function of the spectral phase is directly measured, but complete phase retrieval requires an integration or concatenation step and some assumptions on the pulse duration and exact spectral shape. Experimentally, as single-shot implementation of these techniques uses non-collinear harmonic generation, their alignments are complex.

The existence of a reference pulse, with a known spectral phase on a larger bandwidth than the pulse to be measured, hugely simplifies the measurement setup and algorithm by using spectral interferometry [5, 6]. This method is linear, analytic, sensitive and accurate. Unlike the SPIDER technique, neither shear nor harmonic generation is needed. However, to make this measurement self referenced, the reference pulse has to be generated from the pulse itself.

In our technique, hereafter named self-referenced spectral interferometry (SRSI), the reference pulse is ‘self created’ by the combination of an acousto-optic programmable dispersive filter (AOPDF) [7] and a frequency-conserving non-linear optical effect. In Sect. 2 we investigate both theoretically and experimentally the creation mechanism and the spectral characteristics of the self-created reference pulse. In Sect. 3 we present the method used to extract the input pulse’s spectral amplitude and phase. Finally, in Sect. 4 we propose an application of this technique to the pulse optimization of a chirped pulse amplification (CPA) laser chain.

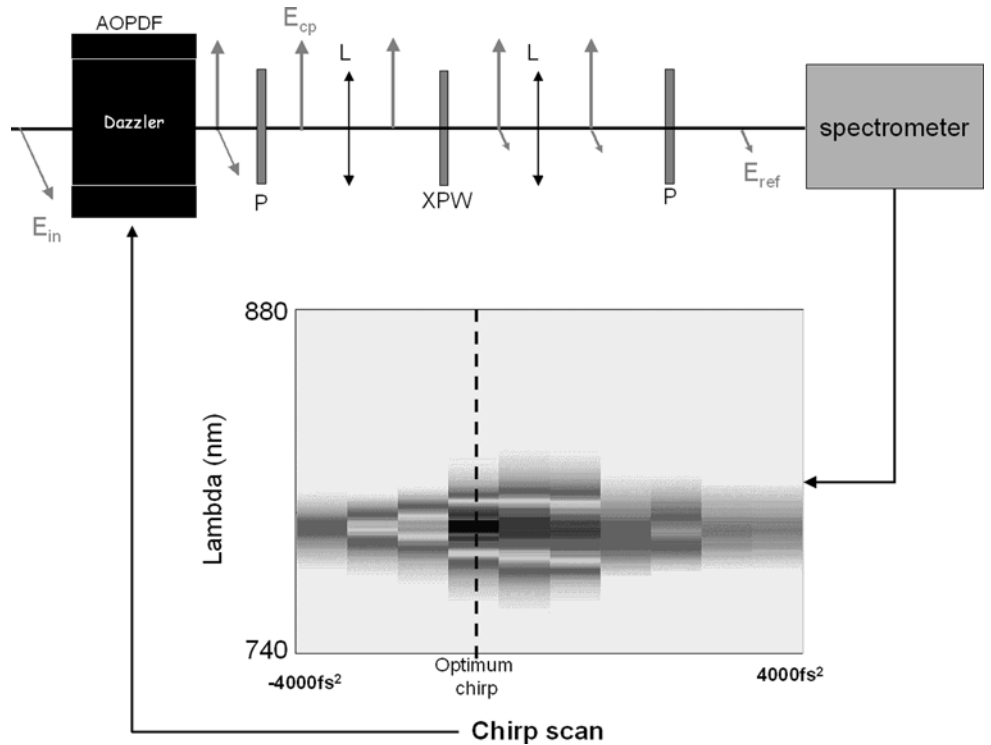
2 Reference pulse creation

In the spatial domain, an input beam can be spatially filtered to obtain a beam with a larger beam diameter and a flatter

T. Oksenhendler (✉) · S. Coudreau · N. Forget · V. Crozatier ·
S. Grabielle · R. Herzog · D. Kaplan
FASTLITE, Centre Scientifique d’Orsay, Bât. 503, Plateau
du Moulon, BP45, 91401 Orsay, France
e-mail: thoksen@fastlite.com
Fax: +33-1-69333098

S. Grabielle · O. Gobert
CEA/SPAM/SLIC, CEA Saclay, 91191 Gif/Yvette, France

Fig. 1 Reference pulse optimization first step: chirp correction (grey arrows indicate the polarization of light, L: lens, P: polarizer, XPW: non-linear crystal)



phase. By analogy, a reference pulse in the spectral domain can be obtained by temporally filtering the input pulse. In the femtosecond domain, the temporal filter is provided by a non-linear effect. For reasons of compactness, simplicity, colinearity and achromaticity, a particularly well-suited non-linear effect is cross-polarized wave generation (XPW) [8]. A XPW generated signal presents, to the first order, a cubic dependence on the time-dependent intensity of the input signal. As demonstrated by Jullien et al. [9], this cubic dependence reduces the input second order spectral phase (chirp) by a factor of nine: it acts as a pinhole, filtering in the time domain. For higher order spectral phase, the filtering is even more efficient. For a chirp-free pulse, duration shortening also broadens the spectrum. Thus, if an initial input pulse has no significant chirp, the XPW generated signal can be considered as an approximately flat reference pulse.

The reference pulse is therefore obtained in two steps: a coarse compression first eliminates the chirp and then a fine compression damps higher order in the spectral phase.

Coarse compression is obtained by optimizing the chirp via maximization of the non-linear signal intensity. The experimental setup is described in Fig. 1. The pulse shaper is used to scan the chirp values (chirp scan) and a spectrometer records the XPW spectrum for every chirp value. The chirp that maximizes the non-linear signal corresponds to the correction of the input pulse's chirp. Once the chirp is eliminated, the pulse is short enough to be efficiently temporally filtered by the XPW effect.

The second step of the optimization process relies on the pulse cleaning properties of the XPW effect. Because the XPW efficiency scales with the cube of the time intensity, the XPW pulse duration is shorter and its spectrum is broader than the fundamental pulse. Let $E_{CP}(t)$ and $E_{CP}(\omega)$ be respectively the time and spectral amplitudes of the compensated pulse (pulse after AOPDF). Let also $E_{ref}(t)$ and $E_{ref}(\omega)$ be those of the reference pulse (pulse after AOPDF and XPW generation). In a first approximation, $E_{ref}(t)$ and $E_{CP}(t)$ are linked by

$$E_{ref}(t) \propto |E_{CP}(t)|^2 E_{CP}(t). \quad (1)$$

The phase difference between $E_{CP}(\omega)$ and $E_{ref}(\omega)$ is measured by Fourier-transform spectral interferometry (FTSI) [10]. As depicted in Fig. 2, a calcite plate is used to introduce an optical delay τ between E_{ref} and E_{CP} . The signal measured by the spectrometer can then be expressed as

$$\begin{aligned} S(\omega) &= |E_{ref}(\omega) + E_{CP}(\omega)e^{i\omega\tau}|^2 \\ &= |E_{ref}(\omega)|^2 + |E_{CP}(\omega)|^2 + f(\omega)e^{i\omega\tau} \\ &\quad + f^*(\omega)e^{-i\omega\tau}, \end{aligned} \quad (2)$$

where $f(\omega) = E_{ref}(\omega)E_{CP}^*(\omega)$ is the interference term between the compensated and reference pulses. FTSI starts by taking the inverse Fourier transform of the measured spec-

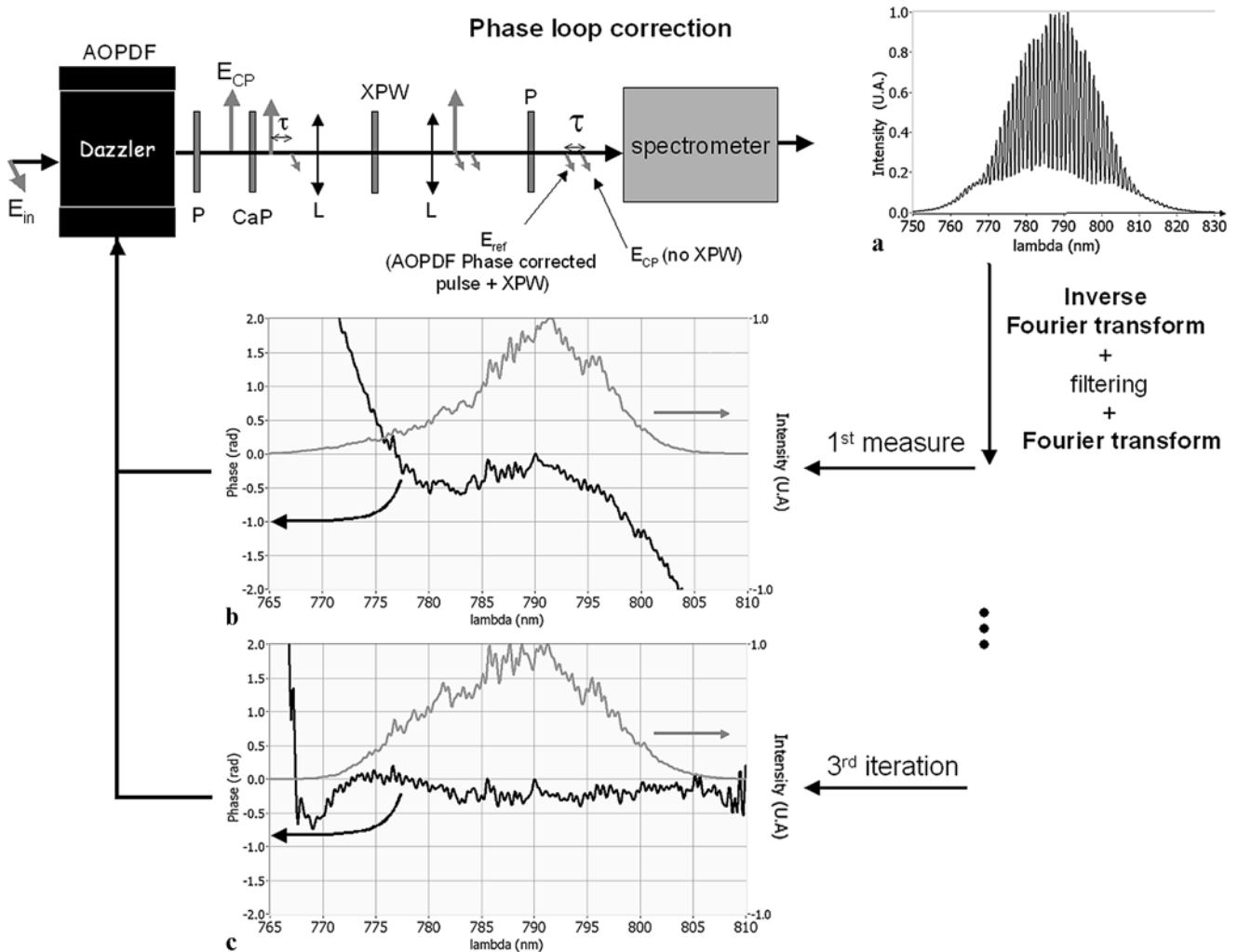


Fig. 2 Reference pulse optimization second step: higher order term correction by iterations. (a) Measured interferogram, (b) 1st measured spectral amplitude (grey) and phase (black), (c) 3rd iteration spectral

amplitude (grey) and phase (black). CaP: calcite plate, L: focusing and recollimating lenses, P: polarizers

trum, which is written

$$\begin{aligned} F.T.^{-1}[S](t) = & E_{\text{ref}}^*(-t) \otimes E_{\text{ref}}(t) + E_{\text{CP}}^*(-t) \otimes E_{\text{CP}}(t) \\ & + f(t - \tau) + f^*(-t - \tau). \end{aligned} \quad (3)$$

In this expression, the first two terms correspond to the field autocorrelation functions of each pulse and are thus centered around $t = 0$. The third and fourth terms are the correlation functions shifted by τ and are centered at $t = \tau$ and $t = -\tau$, respectively. If the value of τ is large enough to avoid any overlap between the terms, $f(t - \tau)$ can be extracted by numerically filtering out the other terms. Fourier transforming back into the frequency domain then yields $f(\omega)e^{i\omega\tau}$, whose phase and amplitude are

$$\arg[f(\omega)e^{i\omega\tau}] = \varphi_{\text{ref}}(\omega) - \varphi_{\text{CP}}(\omega) + \omega\tau, \quad (4)$$

$$|f(\omega)e^{i\omega\tau}| = |E_{\text{ref}}(\omega)| |E_{\text{CP}}(\omega)|. \quad (5)$$

Since the reference pulse is only approximately known, the spectral phase difference measured is, at most, an estimation of the spectral phase of the compensated pulse. However, this phase estimation can be used to further correct the input pulse using the pulse shaper. By iterating this procedure, the compensated pulse converges to a pure flat phase pulse after only a few loops (three for example in Fig. 2).

Flattening the spectral phase shortens the filtered pulse and tends to enlarge the spectral width of the XPW pulse (i.e. the reference pulse) with respect to the pulse to be characterized, a feature perfectly adapted to spectral interferometry: the reference pulse has a flatter phase and a broader spectrum than the input pulse. Besides, since the maximum spectral broadening is reached for a flat phase input, this enlargement is a very efficient criterion of convergence.

The experimental results shown in Figs. 1 and 2 were obtained on the 20 Hz, 50 fs (20 nm) multi-mJ LUCA

laser chain at the CEA. About 10 μJ of energy was sampled from the main beam. The input pulse is first shaped by the AOPDF. The diffracted beam is selected by a polarizer to select the compensated pulse. The shaping consists in a pure phase shaping. This pulse is focused by a first lens ($f = 100 \text{ mm}$) onto the non-linear XPW crystal (1-mm-thick LiF crystal cut along the [100] direction) and recollimated with a second lens ($f = 100 \text{ mm}$). A second polarizer selects the XPW generated pulse. For the second step optimization, the necessary optical delayed pulse replica (compensated pulse) for spectral interferometry was obtained by inserting a suitable calcite plate ($\tau = 1.8 \text{ ps}$).

The interferogram shown in Fig. 2a illustrates the broadening of the spectrum by the XPW filtering. The reference pulse has indeed a larger bandwidth (750–825 nm) than the compensated one (770–805 nm). This is shown by the absence of fringes on the sides. This broadening is also visible in the spectrum measured after the 3rd iteration (Fig. 2c).

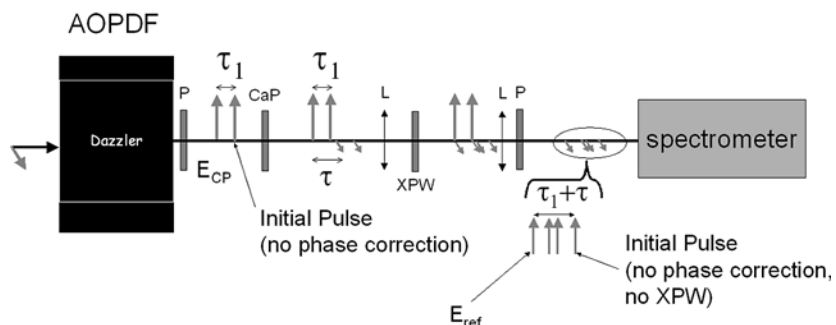
In this experiment the procedure was applied to a pulse containing a significant 3rd order of spectral phase and a mix of 2nd and 4th orders of spectral phase. The figure shows the phase of the corrected pulse obtained after the coarse chirp optimization (1st measured) and the final phase (after three iterations) with deviations of less than 0.2 radians over the complete spectrum.

3 Determination of the input pulse characteristics

3.1 Spectral phase

Once the reference pulse optimization has been accomplished, the characteristics of the input pulse can be directly obtained by relying on the quantitative nature of the AOPDF pulse shaping [11]. The spectral phase added to obtain an output flat phase yields the initial spectral phase to be measured. Small fluctuations of the phase can then be directly inferred from the spectral interferometry on a shot-to-shot basis (Fig. 2).

Fig. 3 Spectral interferometry between reference pulse and input pulse, τ_1 : delay between input pulse and compensated pulse, τ : delay introduced by the calcite plate (CaP)



Without any modification of the optical setup, it is also possible to measure the complete spectral phase by using an extra pulse at the output of the pulse shaper (Fig. 3). This added pulse is a replica of the input pulse without any modification except a time delay τ_1 . At the input of the spectrometer, four pulses are present but only two have the maximum optical delay separation in time. By filtering the signal in the time domain around this delay, we directly obtain the spectral phase of the initial pulse.

This direct estimation of the spectral phase, which does not rely on the correction applied by the pulse shaper, is also single shot. Nevertheless, this method requires two different pulses at the output of the pulse shaper with the same spectrum, which implies an amplitude modulation. This amplitude modulation may limit the capability of this method (cf. pulse optimization of a CPA laser chain).

3.2 Spectral intensity

The spectral intensity (spectrum) can be recovered either by measuring the spectrum directly or by using the interferogram.

In the first case, the polarizer is simply rotated to select only the compensated pulse, and this is a classical spectrum measurement.

In the second case, two methods can be applied to recover the spectrum of each pulse. The first one is based on a blind iterative algorithm using the relationship between these two pulses: the reference pulse is the compensated pulse temporally filtered by XPW. Its electric field is calculated from the compensated pulse signal by simulating the XPW effect in the time domain with (1). Initially, the reference pulse is assumed to be a Dirac peak function in the time domain. The compensated pulse is then extracted from the interference term and used to calculate the reference pulse, which is then used to recalculate the compensated pulse. Iterating this loop, the two pulses converge rapidly to their final value (<10 iterations).

The second method is analytical and uses the other terms of the spectral interferometry signal (2). In the time domain, the two field autocorrelation functions of each pulse can

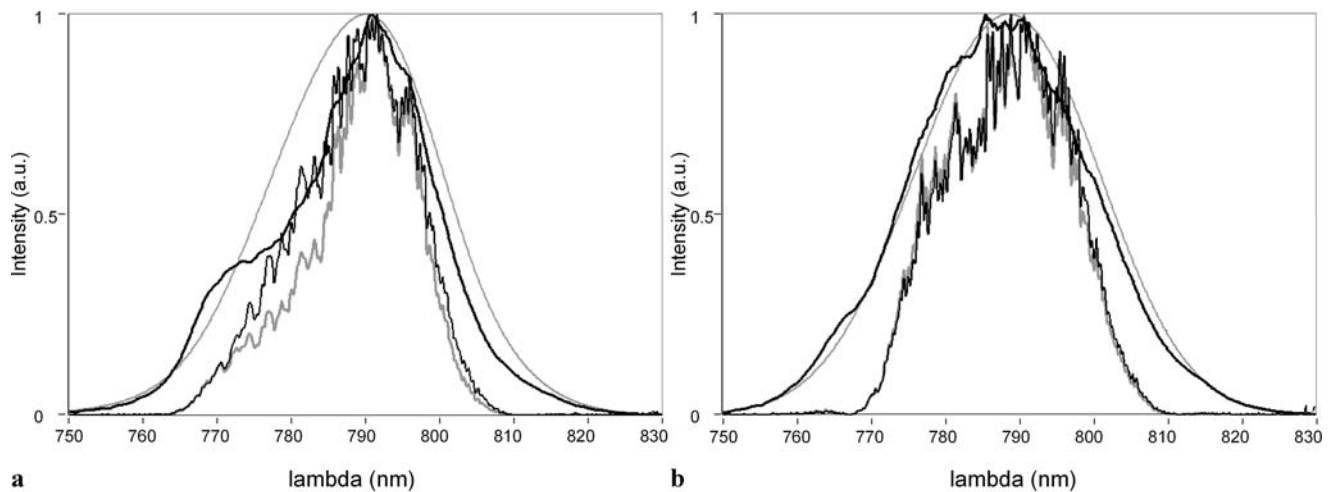


Fig. 4 Spectral intensities of compensated pulse and reference pulse recovered by the iteration (grey) and analytic (black) algorithms for (a) 1st measured, (b) 3rd iteration

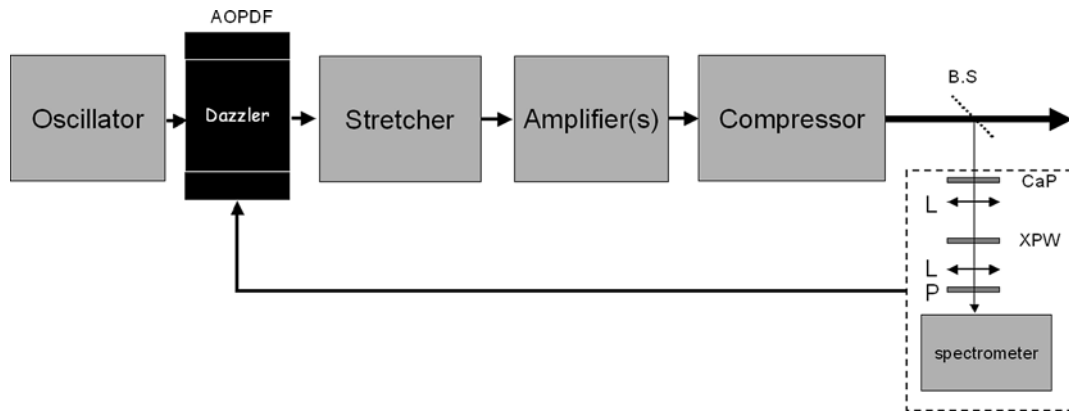


Fig. 5 CPA laser pulse optimization (B.S.: beam sampler)

be numerically filtered as the interference term. An inverse Fourier transform toward the frequency domain then yields

$$S_0(\omega) = |E_{\text{ref}}(\omega)|^2 + |E_{\text{CP}}(\omega)|^2. \quad (6)$$

Both pulse spectra are directly obtained by combining this signal with the amplitude of the interference signal $|f(\omega)| = |E_{\text{ref}}(\omega)||E_{\text{CP}}(\omega)|$:

$$\begin{aligned} |E_{\text{ref}}(\omega)| &= \frac{1}{2} \left(\sqrt{(S_0(\omega) + 2|f(\omega)|)} \right. \\ &\quad \left. + \sqrt{(S_0(\omega) - 2|f(\omega)|)} \right), \\ |E_{\text{CP}}(\omega)| &= \frac{1}{2} \left(\sqrt{(S_0(\omega) + 2|f(\omega)|)} \right. \\ &\quad \left. - \sqrt{(S_0(\omega) - 2|f(\omega)|)} \right). \end{aligned} \quad (7)$$

These two methods can be used to cross check the results (cf. Fig. 4), the quality of the reference pulse and therefore of the measurement.

4 Pulse optimization of a CPA laser chain

SRSI can be applied to pulse optimization in a CPA laser chain in which the pulse shaper is inserted before the amplifier. The non-linearities in the amplification process prohibit the use of amplitude modulation, in the pulse shaper, to measure pulse characteristics [12, 13]. The principle of the measurement illustrated by Fig. 2 is a phase-only modulation, fully compatible with a CPA laser chain (Fig. 5).

The optimization procedure to get the self-created reference pulse is exactly the same. Once the optimization is achieved, the spectral phase fluctuation measurement can also be made single shot.

5 Conclusion

This new femtosecond pulse characterization method has the advantages of spectral interferometry (sensitivity, direct algorithm, precision, resolution, dynamic and large temporal

range), without the need of an external reference. The self-created reference is obtained through a few-loop process (less than 10 different measurement points required) making this method fast and robust. The ability to cross check the results with the pulse shaper enhances the robustness. It allows us to measure small spectral phase evolution (less than 10% evolution of the pulse) in single-shot measurements. Promising developments of this method for two-dimensional characterization and UV pulse measurement are under study.

References

1. V. Wong, I. Walmsley, JOSA B **12**, 1491 (1995)
2. D.J. Kane, R. Trebino, IEEE J. Quantum Electron. **29**, 571 (1993)
3. C. Iaconis, I.A. Walmsley, Opt. Lett. **23**, 792 (1998)
4. D.J. Kane, JOSA B **25**, A120 (2008)
5. Cl. Froehly, A. Lacourt, J.Ch. Viénot, Nouv. Rev. Opt. **4**, 183 (1973)
6. C. Dorrer, M. Joffre, C. R. Acad. Sci. Paris Sér. IV **2**, 1415 (2001)
7. F. Verluise, V. Laude, Z. Cheng, C. Spielmann, P. Tournois, Opt. Lett. **25**, 575 (2000)
8. N. Minkovski, G.I. Petrov, S.M. Saltiel, O. Albert, J. Etchepare, JOSA B **21**, 1659 (2004)
9. A. Jullien, L. Canova, O. Albert, D. Boschetto, L. Antonucci, Y.-H. Cha, J.P. Rousseau, P. Chaudet, G. Chériaux, J. Etchepare, S. Kourtev, N. Minkovski, S.M. Saltiel, Appl. Phys. B **87**, 595 (2007)
10. L. Lepetit, G. Chériaux, M. Joffre, JOSA B **12**, 2467 (1995)
11. T. Oksenhendler, R. Herzog, P. Rousseau, O. Gobert, M. Perdrix, P. Meynadier, *CLEO 2003, CWEI*, pp. 1176–1177
12. X. Liu, R. Wagner, A. Maksimchuk, E. Goodman, J. Workman, D. Umstadter, A. Migus, Opt. Lett. **20**, 1163 (1995)
13. M. Boyle, A. Thoss, N. Zhavaronko, G. Korn, D. Kaplan, T. Oksenhendler, *CLEO 2001, CWA6*, p. 269